Influence of charge asymmetry and isospin-dependent cross section on elliptical flow

Anupriya Jain and Suneel Kumar*
School of Physics and Material Science, Thapar University, Patiala 147004, Punjab, India

Rajeev K. Puri
Department of Physics, Panjab University, Chandigarh 160014, India

(Received 16 September 2011; revised manuscript received 14 December 2011; published 12 June 2012)

Using the isospin-dependent quantum molecular dynamics model, we study the effect of charge asymmetry and isospin-dependent cross section on different aspects of elliptical flow. Simulations are carried out for the reactions of ${}^{124}_{z_1}\mathrm{X}_n + {}^{124}_{z_1}\mathrm{X}_n$, where $z_1 = 47, 50, 53, 57$, and 59 and ${}^{40}_{z_2}\mathrm{Y}_n + {}^{40}_{z_2}\mathrm{Y}_n$, where $z_2 = 14, 16, 18, 21$ and 23. Our study shows that the elliptical flow depends strongly on the nature of the cross section. Transition energy, on the other hand, is unaffected by the neutron content.

DOI: 10.1103/PhysRevC.85.064608 PACS number(s): 25.70.Pq, 21.65.Ef

I. INTRODUCTION

Heavy-ion collisions (HICs) at intermediate energies provide a unique possibility for studying the properties of nuclear matter under extreme conditions [1]. Considerable progress has been made in the last few years to determine the equation of state (EOS) of nuclear matter from heavy-ion reactions [2]. As noted, collective flow and its various variants are the backbone of all such studies. Significant theoretical and experimental efforts have been made recently to study collective flow, especially elliptical flow in HICs [3]. As reported by many authors [4], elliptic flow is quantified by the second-order Fourier coefficient obtained from the azimuthal distribution of the detected particles at mid-rapidity as

$$\frac{dN}{d\phi} = p_0(1 + 2v_1 \cos\phi + 2v_2 \cos 2\phi + \ldots). \tag{1}$$

Here ϕ stands for the azimuthal angle of the emitted particle. Note that the positive values of $\langle \cos 2\phi \rangle$ reflect a preferential in-plane emission. On the other hand, negative values denote preferential out-of-plane emission of nuclear matter.

One should also keep in mind that the scattering cross section depends crucially on the isospin content. The neutron-proton cross section ($\sigma_{np}^{\mathrm{free}}$) in free space is higher compared to the corresponding proton-proton ($\sigma_{pp}^{\mathrm{free}}$) or neutron-neutron ($\sigma_{nn}^{\mathrm{free}}$) cross section. The transition matrices of the isospin $T = 1$ and $T = 0$ channels contribute to this difference. For the neutron-proton cross section both isosinglet and isotriplet channels contribute whereas only the isotriplet channel is responsible for the proton-proton and neutron-neutron cross sections. The neutron-proton cross section is about three times larger compared to proton-proton and neutron-neutron cross sections.

Recently, Yan *et al.* [6] studied the scaling of anisotropic flows (v_2 and v_4) of light charged clusters. They showed [6] that there exists a scaling rule for both anisotropic flow and momentum-space densities for light charged clusters. This behavior was explained in the light of the coalescence mechanism.

On the other hand, Zheng *et al.* [7] studied proton elliptic flow for the reaction of ${}^{48}\mathrm{Ca} + {}^{48}\mathrm{Ca}$ at energies from 30 to 100 MeV/nucleon. A transition from positive to negative values of elliptical flow was noted with incident energy. The magnitude of these values was found to depend on both the nuclear EOS as well as the nucleon-nucleon scattering cross section. Zhang and Li [8], on the other hand, investigated elliptic flow in HICs at energies ranging from several tens to several hundreds of MeV/nucleon. A soft nuclear EOS along with incident-energy-dependent in-medium nucleon-nucleon cross sections was needed to describe the excitation function of elliptic flow at intermediate energies.

Note that all these studies were silent about the effect of charge asymmetry and isospin-dependent cross section on elliptical flow. These effects need to be explored in HICs in a systematic manners. We aim to address this problem using the isospin-dependent quantum molecular dynamics (IQMD) [9] model.

II. ISOSPIN-DEPENDENT QUANTUM MOLECULAR DYNAMICS MODEL

Our study is performed within the framework of the isospin-dependent quantum molecular dynamics [9] model, where hadrons propagate with Hamilton equations of motion:

$$\frac{dr_i}{dt} = \frac{d\langle H\rangle}{dp_i}; \quad \frac{dp_i}{dt} = -\frac{d\langle H\rangle}{dr_i}, \tag{2}$$

with

$$\begin{aligned}\langle H\rangle &= \langle T\rangle + \langle V\rangle \\ &= \sum_i \frac{p_i^2}{2m_i} + \sum_i \sum_{j>i} \int f_i(\vec{r}, \vec{p}, t) V^{ij}(\vec{r}', \vec{r}) \\ &\quad \times f_j(\vec{r}', \vec{p}', t) d\vec{r} d\vec{r}' d\vec{p} d\vec{p}'. \end{aligned} \tag{3}$$

*suneel.kumar@thapar.edu

The baryon-baryon potential V^{ij}, in the above relation, reads as

$$V^{ij}(\vec{r}'-\vec{r}) = V^{ij}_{Skyrme} + V^{ij}_{Yukawa} + V^{ij}_{Coul} + V^{ij}_{sym}$$
$$= \left[t_1\delta(\vec{r}'-\vec{r}) + t_2\delta(\vec{r}'-\vec{r})\rho^{\nu-1}\left(\frac{\vec{r}'+\vec{r}}{2}\right)\right]$$
$$+ t_3\frac{\exp(|\vec{r}'-\vec{r}|/\mu)}{(|\vec{r}'-\vec{r}|/\mu)} + \frac{Z_iZ_je^2}{|\vec{r}'-\vec{r}|}$$
$$+ t_6\frac{1}{\varrho_0}T_3^iT_3^j\delta(\vec{r}_i{}'-\vec{r}_j). \quad (4)$$

Here Z_i and Z_j denote the charges of the ith and jth baryons, and T_3^i and T_3^j are their respective T_3 components (i.e., $1/2$ for protons and $-1/2$ for neutrons). For the density dependence of the nucleon optical potential, standard Skyrme-type parametrizations are employed. The potential part resulting from the convolution of the distribution function with the Skyrme interactions V_{Skyrme} reads as

$$V_{Skyrme} = \alpha\left(\frac{\rho_{int}}{\rho_0}\right) + \beta\left(\frac{\rho_{int}}{\rho_0}\right)^{\delta}, \quad (5)$$

where ρ_{int} is the instantaneous density. Two of the three parameters of the EOS are determined by assuming that, at normal nuclear matter density, the binding energy should be equal to 16 MeV. The compressibility factor is

$$\kappa = 9\rho^2\frac{\partial^2}{\partial\rho^2}\left(\frac{E}{A}\right). \quad (6)$$

The parameter δ determines the stiffness of the EOS. The different values of compressibility give rise to soft (κ = 200 MeV, at smaller value of δ) and hard (κ = 380 MeV, at larger value of δ) equations of state. The Gaussian width L is defined as a description of the interaction range of the particle. As mentioned in Ref. [9], in IQMD the value of the Gaussian width L depends on the mass of the system. For heavier systems, e.g., ${}^{197}_{79}\mathrm{Au}_{118} + {}^{197}_{79}\mathrm{Au}_{118}$, $L = 8.33$ fm^2; for ${}^{124}_{z_1}\mathrm{X}_n + {}^{124}_{z_1}\mathrm{X}_n$, $L = 6.75$ fm^2; and for lighter ones, i.e., ${}^{40}_{z_2}\mathrm{Y}_n + {}^{40}_{z_2}\mathrm{Y}_n$, $L = 4.33$ fm^2. A large number of studies have been performed on the density dependence of the symmetry energy in the recent past. The following equation provides us with the most extensively used parametrizations of the symmetry energy in terms of the nuclear density ρ:

$$E(\rho) = E(\rho_o)(\rho/\rho_o)^{\gamma}. \quad (7)$$

The parameter γ determines the stiffness of the EOS [10–12]. In our calculations, we use $\gamma = 0.66$. The parametrization of the EOS stated above for the exact value of γ is still a challenging task and a topic of vital interest for nuclear physics research in the present decade.

During the propagation, two nucleons are supposed to suffer a binary collision if the distance between their centroid is

$$|r_i - r_j| \leqslant \sqrt{\frac{\sigma_{\mathrm{tot}}}{\pi}}, \quad \sigma_{\mathrm{tot}} = \sigma(\sqrt{s}, \mathrm{type}), \quad (8)$$

where "type" denotes the in-going collision partners (N-N, N-Δ, N-π, ...). In addition, Pauli blocking (of the final state) of baryons is taken into account by checking the phase-space densities in the final states.

III. RESULTS AND DISCUSSION

For the present analysis, simulations are carried out for two different sets of reactions. Twenty-thousand events were simulated for a reaction time of 200 fm/c. For the first case, the total mass of the colliding nuclei is fixed at 124 units and, for the second set, the mass of the colliding nuclei was fixed to be 40 units. In other words, we study the reactions of ${}^{124}_{z_1}\mathrm{X}_n + {}^{124}_{z_1}\mathrm{X}_n$, where ${}^{124}_{z_1}\mathrm{X}_n$ = (${}^{124}_{47}\mathrm{Ag}_{77}$, ${}^{124}_{50}\mathrm{Sn}_{74}$, ${}^{124}_{53}\mathrm{I}_{71}$, ${}^{124}_{57}\mathrm{La}_{67}$, and ${}^{124}_{59}\mathrm{Pr}_{65}$), respectively. The second set corresponds to ${}^{40}_{z_2}\mathrm{Y}_n + {}^{40}_{z_2}\mathrm{Y}_n$, where ${}^{40}_{z_2}\mathrm{Y}_n$ = (${}^{40}_{21}\mathrm{Sc}_{19}$, ${}^{40}_{20}\mathrm{Ca}_{20}$, ${}^{40}_{18}\mathrm{Ar}_{22}$, ${}^{40}_{16}\mathrm{S}_{24}$, and ${}^{40}_{14}\mathrm{Si}_{26}$), respectively. The phase space generated by the IQMD model was then analyzed using the minimum spanning tree (MST) [13] method. The elliptical flow is defined as the average difference between the square of the x and y components of the nucleonic transverse momentum. The importance of the elliptical flow parameter v_n was discussed by Voloshin and Zhang [4], while the term elliptical flow was first introduced in 1997 by Sorge [14]. He studied the elliptical flow in noncentral Au + Au (E = 11.7 GeV/nucleon) collisions and indicated the role of pressure and the EOS in elliptical flow. Mathematically, it can be written as [15]

$$\langle v_2\rangle = \langle \mathrm{Cos}\,2\phi\rangle = \left\langle\frac{p_x^2 - p_y^2}{p_x^2 + p_y^2}\right\rangle, \quad (9)$$

where p_x and p_y are the x and y components of the momenta. As noted in Ref. [15], a positive value of elliptical flow describes the eccentricity of an ellipse-like distribution and indicates in-plane enhancement of the particle emission. On the other hand, a negative value of $\langle v_2\rangle$ denotes squeeze-out effects perpendicular to the reaction plane [15]. Obviously, a zero value corresponds to an isotropic distribution. Generally, for a meaningful understanding, $\langle v_2\rangle$ is extracted from the mid-rapidity region only. Naturally, the mid-rapidity region ($-0.1 \leqslant \frac{Y_{c.m}}{Y_{beam}} \leqslant 0.1$) corresponds to the collision (participant) zone and hence signifies compressed matter. On the other hand, $\frac{Y_{c.m}}{Y_{beam}} \neq 0$ corresponds to the spectator zone, $\frac{Y_{c.m}}{Y_{beam}} < -0.1$ corresponds to targetlike (TL) matter, and $\frac{Y_{c.m}}{Y_{beam}} > 0.1$ corresponds to projectilelike (PL) matter. The rapidity is defined as [16]

$$Y_{c.m.} = \frac{1}{2}\ln\left(\frac{E + p_z}{E - p_z}\right), \quad (10)$$

where E is the energy and p_z is the z component of the momentum.

To study the effect of charge asymmetry on the elliptical flow as a function of $\langle p_t\rangle$, [where $\langle p_t\rangle$ is the transverse momentum of the particle and is given by $p_t = \sqrt{(p_x^2 + p_y^2)}$], we display in Figs. 1 and 2 the final-state elliptical flow for free nucleons (FNs) ($A = 1$) [(a) and (d)], light-mass fragments (LMFs) ($2 \leqslant A \leqslant 4$) [(b) and (e)], and intermediate-mass fragments (IMFs) ($5 \leqslant A \leqslant A_{\mathrm{tot}}/6$) [(c) and (f)] at an incident energy $E = 50$ MeV/nucleon (left panel) and $E = 100$ MeV/nucleon (right panel) for the reactions of ${}^{124}_{z_1}\mathrm{X}_n + {}^{124}_{z_1}\mathrm{X}_n$, where $z_1 = 47$ and 59 (in Fig. 1) and ${}^{40}_{z_2}\mathrm{Y}_n + {}^{40}_{z_2}\mathrm{Y}_n$, where $z_2 = 14$ and 20 (in Fig. 2) for isospin-dependent cross section ($\sigma_{np} = 3\sigma_{nn} = 3\sigma_{pp}$). Here elliptical flow is summed over all rapidity bins (which include the participant as

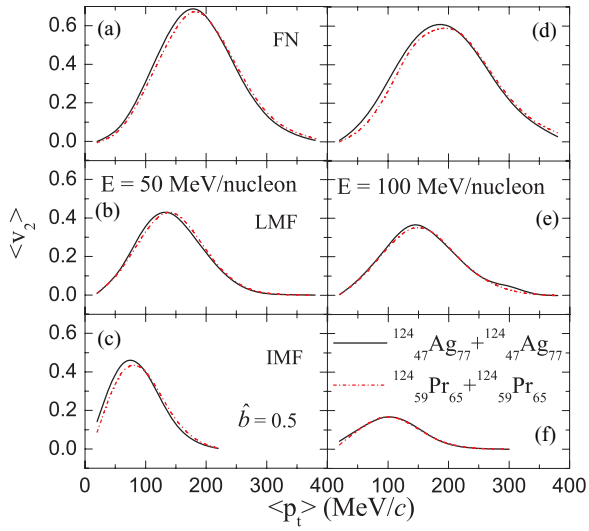

FIG. 1. (Color online) Transverse momentum dependence of the elliptical flow summed over the entire rapidity distribution for two different reactions at an incident energy of 50 (left) and 100 (right) MeV/nucleon.

well as spectator zones, i.e., $-1.75 \leqslant \frac{Y_{c.m.}}{Y_{beam}} \leqslant 1.75$, in 15 bins with bin width of 0.25 each). Figures 1 and 2 reveal the following:

(a) A Gaussian shape is obtained for $\langle v_2 \rangle$ in all cases. Note that the elliptical flow is integrated over the entire rapidity range.

(b) The peak of the Gaussian shifts toward lower values of $\langle p_t \rangle$ for heavier fragments. This is because the FNs and LMFs feel the mean field directly, while heavy fragments have weaker sensitivity [17,18].

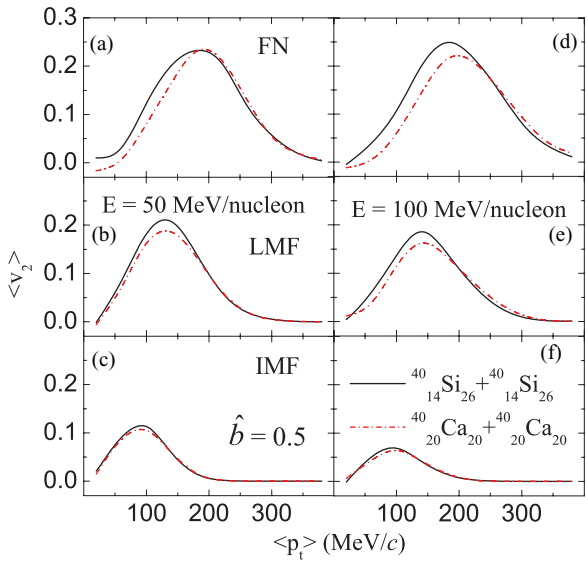

FIG. 2. (Color online) Transverse momentum dependence of the elliptical flow summed over the entire rapidity distribution for two different reactions at an incident energy of 50 (left panel) and 100 MeV/nucleon (right panel).

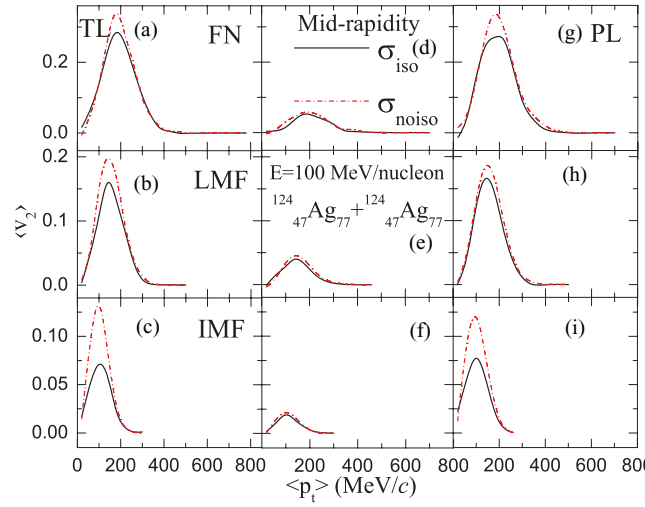

FIG. 3. (Color online) Transverse momentum dependence of the elliptical flow at $E = 100$ MeV/nucleon for two different cross sections.

(c) The neutron-rich systems $^{124}_{47}Ag_{77} + ^{124}_{47}Ag_{77}$ and $^{40}_{14}Si_{26} + ^{40}_{14}Si_{26}$ exhibit weaker squeeze-out flow compared to the neutron-deficient reactions $^{124}_{59}Pr_{65} + ^{124}_{59}Pr_{65}$ and $^{40}_{20}Ca_{20} + ^{40}_{20}Ca_{20}$. Our findings are in agreement with Ref. [17] where a neutron-rich system was found to exhibit weaker squeeze-out flow.

To study the effect of isospin dependence of the cross section and charge asymmetry on the elliptical flow, we display in Figs. 3–6 the transverse momentum dependence of the elliptical flow for the reactions of $^{124}_{47}Ag_{77} + ^{124}_{47}Ag_{77}$, $^{124}_{59}Pr_{65} + ^{124}_{59}Pr_{65}$, $^{40}_{14}Si_{26} + ^{40}_{14}Si_{26}$, and $^{40}_{20}Ca_{20} + ^{40}_{20}Ca_{20}$. We divide total elliptical flow into contributions from TL [(a), (b), and (c)], mid-rapidity [(d), (e), and (f)], and PL [(g), (h), and (i)] particles at $E = 100$ MeV/nucleon. Panels (a), (d), and (g) represent the FNs, (b), (e), and (h) represent the LMFs,

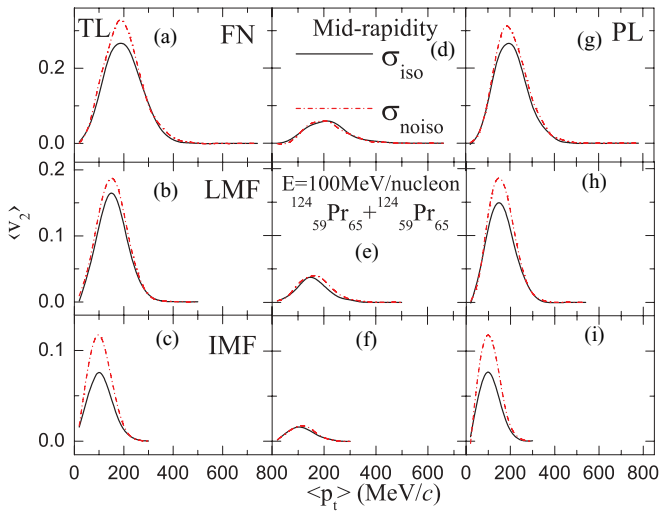

FIG. 4. (Color online) Same as Fig. 3 but for the reaction $^{124}_{59}Pr_{65} + ^{124}_{59}Pr_{65}$.

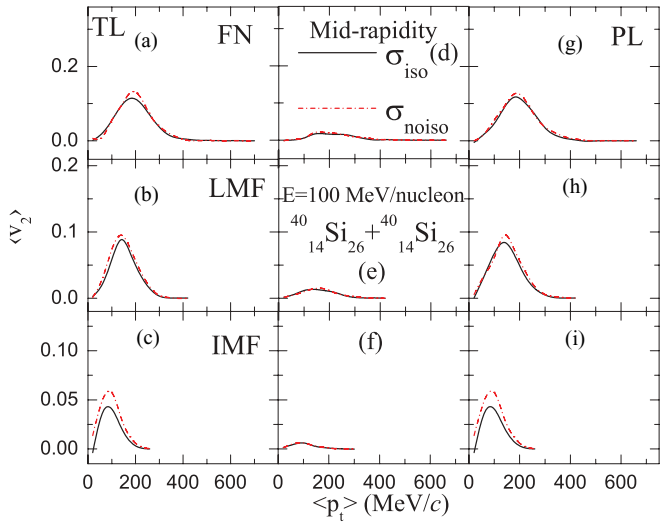

FIG. 5. (Color online) Same as Fig. 3 but for the reaction $^{40}_{14}Si_{26} + ^{40}_{14}Si_{26}$.

and (c), (f), and (i) represent the IMFs. These figures reveal following points:

(a) $\langle v_2 \rangle$ is sensitive to different nucleon-nucleon cross sections. Weaker squeeze-out flow is observed in the case of an isospin-independent cross section ($\sigma_{np} = \sigma_{nn} = \sigma_{pp}$). This happens because, in the case of an isospin-dependent cross section, the neutron-proton cross section is three times larger compared to the neutron-neutron and proton-proton cross sections (i.e., $\sigma_{np} = 3\sigma_{nn} = 3\sigma_{pp}$) [9], which will enhance binary collisions. These findings are in agreement with Ref. [19].

(b) For the mid-rapidity region ($-0.1 \leqslant \frac{Y_{c.m.}}{Y_{beam}} \leqslant 0.1$), little influence is observed for the isospin-dependent cross section. This happens because this zone includes very few nucleons. Moreover, this zone corresponds to the collision (participant) zone, and thus a violent collision phase occurs in this zone, and so the isospin-dependent cross section is not visible in this zone. Moreover, the particle production mechanism in the projectile-like and target-like regions is evaporation because we are taking the reaction time at 200 fm/c.

(c) In the case of IMFs, the difference between the two cross sections is larger compared to those of FNs and LMFs. This happens because the FNs and LMFs are produced from the participant zone and, as stated above, due to the occurrence of the violent phase, various cross sections do not vary drastically. On the other hand, IMFs are being produced from the spectator matter. Therefore, any change in binary cross section can have significant effect on the outcome.

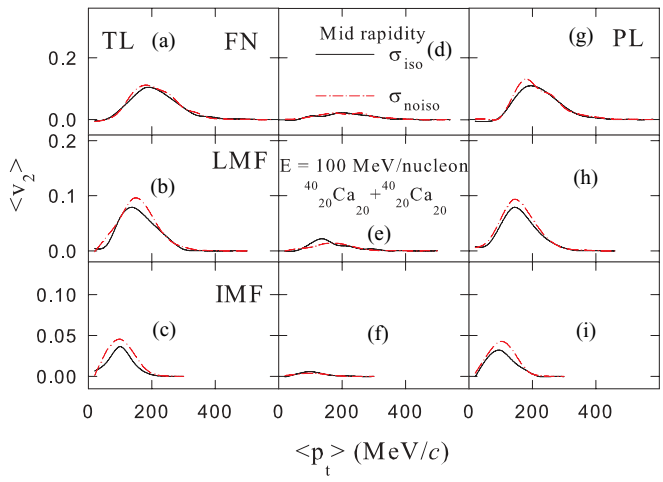

FIG. 6. (Color online) Same as Fig. 3 but for the reaction $^{40}_{20}Ca_{20} + ^{40}_{20}Ca_{20}$.

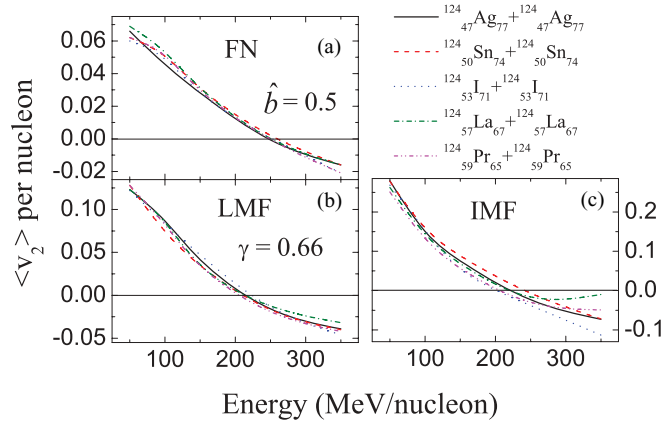

FIG. 7. (Color online) The variation of the elliptical flow with incident energy for the reactions of $^{124}_{z_1}X_n + ^{124}_{z_1}X_n$, where $^{124}_{z_1}X_n = (^{124}_{47}Ag_{77}, ^{124}_{50}Sn_{74}, ^{124}_{53}I_{71}, ^{124}_{57}La_{67}$, and $^{124}_{59}Pr_{65})$.

In Figs. 7–9, we display the variation of the excitation function of elliptical flow $\langle v_2 \rangle$ for FNs [panel (a)], LMFs [panel (b)], and IMFs [panel (c)] for the mid-rapidity region using the same set of reactions considered earlier with the isospin-dependent cross section, for $\gamma = 0.66$ in Figs. 7 and 9 and for $\gamma = 2$ in Fig. 8. We note the following:

(a) The elliptical flow turns negative with beam energy. This is because spectators move faster after $\langle v_2 \rangle$ reaches a minimum value [15,20]. The energy at which this behavior changes is found to decrease with the size of the fragment. This means that the flow of the heavier fragments is larger

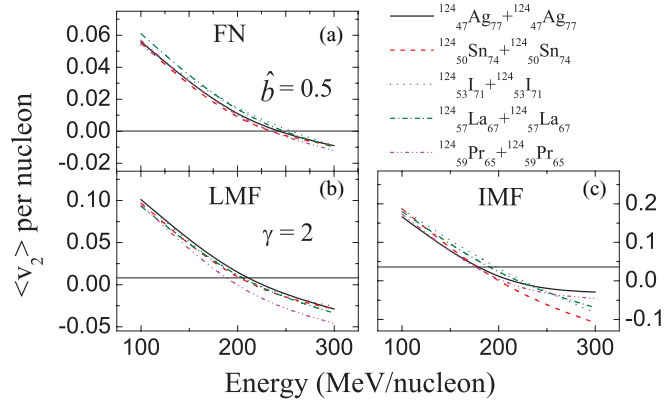

FIG. 8. (Color online) Same as Fig. 7 but for $\gamma = 2$.

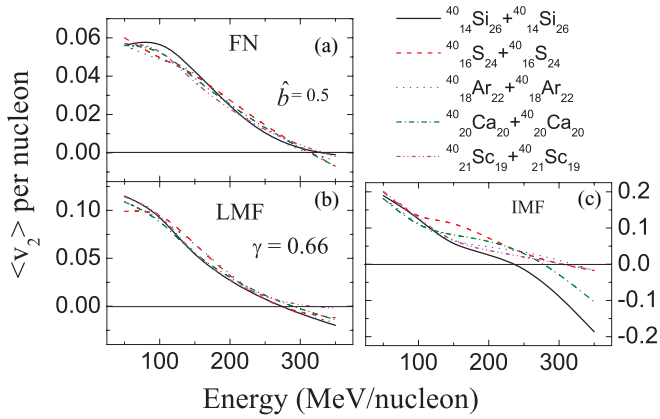

FIG. 9. (Color online) The variation of the elliptical flow with incident energy for the reactions $^{40}_{z_2}Y_n + ^{40}_{z_2}Y_n$, where $^{40}_{z_2}Y_n = (^{40}_{20}Ca_{20}$, $^{40}_{21}Sc_{19}$, $^{40}_{18}Ar_{22}$, $^{40}_{16}S_{24}$, and $^{40}_{14}Si_{26})$.

than that of LMFs and FNs at all beam energies. These findings are in agreement with Ref. [21].

(b) There occurs a transition from in-plane emission to out-of-plane emission. This happens because, at low energies, the mean field dominates. In this work, the rotating nucleus corresponding to the dominating spectator matter contributes toward the directed transverse in-plane flow. At higher incident energies, however, the mean field does not play any significant role. The larger compression produced in the participant zone results in the squeeze-out of the nuclear matter. On the other hand, the elliptical flow, a representative of hot matter and shadowing of the spectator matter, turns negative at relative higher energies.

In other words, the participant zone is primarily responsible for the transition from in-plane to out-of-plane emission. The energy at which this transition is observed is dubbed the transition energy $E_{\rm Trans}$.

To study the effect of the charge asymmetry on the transition energy of FNs [panels (a) and (d)], LMFs [panels (b) and (e)], and IMFs [panels (c) and (f)], we display in Fig. 10 the transition energy as a function of the neutron to proton ratio for FNs [panels (a) and (d)], LMFs [panels (b) and (e)], and IMFs [panels (c) and (f)] for $\gamma = 0.66$ and 2 in the left panels and for $\gamma = 0.66$ in the right panels. From the figures, it is clear that the transition energy remains almost unchanged with the increase in the N/Z ratio of the system. Moreover, the transition energy decreases with the value of γ. Note that the elliptical flow is influenced greatly by the participant matter and thus, in fact, depends on the density reached in a reaction. A larger value of γ corresponds to a larger symmetry energy repulsion around the compressed zone (participant zone). Therefore, elliptical flow tends to be affected by the various forms of the density-dependent symmetry energy. These findings are in agreement with Ref. [22].

To further strengthen our interpretation of the results of elliptical flow $\langle v_2 \rangle$, we display in Fig. 11 a comparison of the theoretical results of elliptical flow with experimental data reported by the INDRA@(GSI + GANIL) Collaboration [23] [panel (a)] for the reaction $^{124}Sn_{50} + ^{124}Sn_{50}$ and with theoretical results [20] [panels (b) and (c)] for the reaction

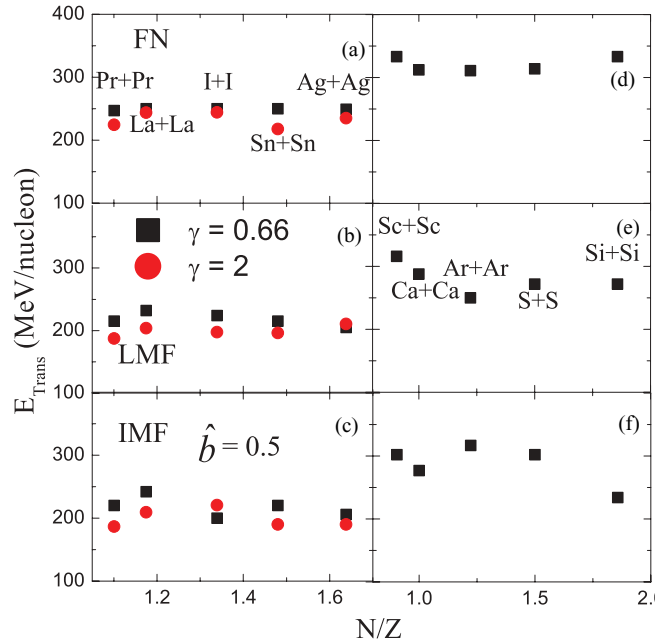

FIG. 10. (Color online) Transition energies ($E_{\rm Trans}$ in MeV/nucleon) as a function of N/Z ratio for FNs [panels (a) and (d)], LMFs [panels (b) and (e)], and IMFs [panels (c) and (f)].

$^{112}Sn_{50} + ^{112}Sn_{50}$. Here simulations were performed with $\sigma_{\rm iso}$ reduced by 20%. The choice of the reduced cross section has also been motivated by Ref. [24] as well as many previous studies [25]. It is worth mentioning that the results with the above choice of cross section are in good agreement with the experimental data of Ref. [23] at higher energies but a large difference is observed at lower energies. This can be due to the experimental filters, which are not accessible to us. Moreover, in panels (b) and (c), the results are not in good agreement with the theoretical results. This is because, in Ref. [20], the

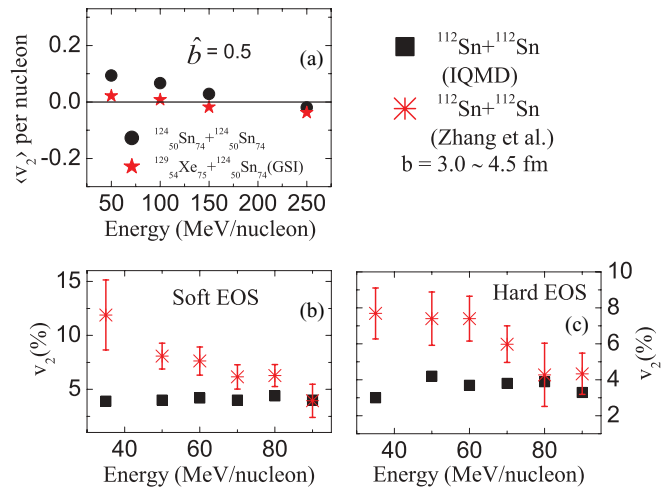

FIG. 11. (Color online) (a) Comparison of $\langle v_2 \rangle$ between theoretical and experimental measurements extracted by the INDRA@(GSI + GANIL) Collaboration for the reaction $^{124}_{50}Sn_{74} + ^{124}_{50}Sn_{74}$. (b) and (c) Comparison of our results with theoretical results of Zhang *et al.* [20] for the reaction of $^{112}_{50}Sn_{62} + ^{112}_{50}Sn_{62}$.

percentage of $\langle v_2 \rangle$ is plotted for all the nucleons, but in our calculations we have plotted the percentage of $\langle v_2 \rangle$ for FNs only.

IV. SUMMARY

Using the isospin-dependent quantum molecular dynamics model, we have studied the effect of charge asymmetry and isospin-dependent cross section on different aspects of elliptical flow. Here simulations have been carried out for the reactions of ${}^{124}_{z_1}\mathrm{X}_n + {}^{124}_{z_1}\mathrm{X}_n$, where $z_1 = 47$, 50, 53, 57, and 59 and ${}^{40}_{z_2}\mathrm{Y}_n + {}^{40}_{z_2}\mathrm{Y}_n$, where $z_2 = 14$, 16, 18, 20, and 21. Our study shows that (a) elliptical flow depends strongly on the isospin dependence of the cross section, (b) the transition energy remains almost constant for various neutron to proton ratios, and (c) the comparison with experimental data of the INDRA@(GSI + GANIL) Collaboration supports our findings.

Moreover, our results for ${}^{40}_{z_2}\mathrm{Y}_n + {}^{40}_{z_2}\mathrm{Y}_n$ will be of great use for experimentalists working at SCC500 at VECC Kolkata, India, in the future.

ACKNOWLEDGMENT

This work has been supported by a grant from the university grant commission (UGC), Government of India [Grant No. 39-858/2010(SR)].

[1] B. A. Li, C. M. Ko, and W. Bauer, Int. J. Mod. Phys. E **7**, 147 (1998).
[2] H. Stocker and W. Greiner, Phys. Rep. **137**, 277 (1986).
[3] J. Lukasik *et al.*, Phys. Lett. B **608**, 223 (2005).
[4] S. Voloshin and Y. Zhang, Z. Phys. C **70**, 665 (1996).
[5] B. A. Li, L. W. Chen, and C. M. Ko, Phys. Rep. **464**, 113 (2008).
[6] T. Z. Yan *et al.*, Phys. Lett. B **638**, 50 (2006).
[7] Y. M. Zheng, C. M. Ko, B. A. Li, and B. Zhang, Phys. Rev. Lett. **83**, 2534 (1999).
[8] Y. Zhang and Z. Li, Phys. Rev. C **74**, 014602 (2006).
[9] C. Hartnack, R. K. Puri, J. Aichelin, J. Konopka, S. A. Bass, H. Stocker, and W. Greiner, Eur. Phys. J. A **1**, 151 (1998); S. A. Bass, C. Hartnack, H. Stocker, and W. Greiner, Phys. Rev. C **51**, 3343 (1995).
[10] C. Xu, B. A. Li, and L. W. Chen, Phys. Rev. C **82**, 054607 (2010).
[11] D. V. Shetty, S. J. Yennello, and G. A. Souliotis, Phys. Rev. C **76**, 024606 (2007).
[12] Y. Zhang, P. Danielewicz, M. Famiano, Z. Li, W. G. Lynch, and M. B. Tsang, Phys. Lett. B **664**, 145 (2008).
[13] J. Aichelin, Phys. Rep. **202**, 233 (1991); R. K. Puri, C. Hartnack, and J. Aichelin, Phys. Rev. C **54**, R28 (1996).
[14] H. Sorge, Phys. Rev. Lett. **78**, 2309 (1997).
[15] A. Andronic *et al.*, Nucl. Phys. A **679**, 765 (2001); Phys. Lett. B **612**, 173 (2005).
[16] D. T. Khoa, N. Ohtsuka, M. A. Matin, A. Faessler, S. W. Huang, E. Lehmann, and R. K. Puri, Nucl. Phys. A **548**, 102 (1992).
[17] S. Kumar, S. Kumar, and R. K. Puri, Phys. Rev. C **81**, 014611 (2010).
[18] Y. T. Zhi, M. Y. Gang, C. X. Zhou, F. D. Qing, G. Wei, M. C. Wang, S. W. Qing, T. W. Dong, and W. Kun, Chin. Phys. **16**, 2676 (2007).
[19] J. Liu, W. J. Guo, Y. Z. Xing, and H. Liu, Nucl. Phys. A **726**, 123 (2003).
[20] H. Y. Zhang, W. Q. Shen, Y. G. Ma, X. Z. Cai, D. Q. Fang, L. P. Yu, C. Zhong, and Y. B. Wei, Eur. Phys. J. A **15**, 399 (2002).
[21] H. Y. Zhang, W. Q. Shen, Y. G. Ma, X. Z. Cai, L. P. Yu, C. Zhong, Y. B. Wei, and J. G. Chen, J. Phys. G **28**, 2397 (2002).
[22] K. S. Vinayak and S. Kumar, Eur. Phys. J. A **47**, 144 (2011).
[23] J. Lukasik and W. Trautmann, for the INDRA and ALADIN Collaborations, arXiv:0708.2821v1 [nucl-ex]; J. Lukasik *et al.*, International Workshop on Multifragmentation and Related Topics, Fig. 6, 4–7 Nov., IWM 2007.
[24] S. Gautam, R. Chugh, A. D. Sood, R. K. Puri, C. Hartnack, and J. Aichelin, J. Phys. G **37**, 085102 (2010).
[25] F. Daffin and W. Bauer, arXiv:nucl-th/9809024v1.